Super and sub-Poissonian photon statistics for single molecule spectroscopy

Yong He[1], Eli Barkai[1,2]
[1] *Department of Chemistry and Biochemistry, Notre Dame University, Notre Dame, IN 46556.*
[2] *Department of Physics, Bar Ilan University, Ramat Gan 52900, Israel*
(Dated: February 2, 2008)

We investigate the distribution of the number of photons emitted by a single molecule undergoing a spectral diffusion process and interacting with a continuous wave laser field. The spectral diffusion is modeled based on a stochastic approach, in the spirit of the Anderson-Kubo line shape theory. Using a generating function formalism we solve the generalized optical Bloch equations, and obtain an exact analytical formula for the line shape and Mandel's Q parameter. The line shape exhibits well known behaviors, including motional narrowing when the stochastic modulation is fast, and power broadening. The Mandel parameter, describing the line shape fluctuations, exhibits a transition from a Quantum sub-Poissonian behavior in the fast modulation limit, to a classical super-Poissonian behavior found in the slow modulation limit. Our result is applicable for weak and strong laser field, namely for arbitrary Rabi frequency. We show how to choose the Rabi frequency in such a way that the Quantum sub-Poissonian nature of the emission process becomes strongest. A lower bound on Q is found, and simple limiting behaviors are investigated. A non-trivial behavior is obtained in the intermediate modulation limit, when the time scales for spectral diffusion and the life time of the excited state, become similar. A comparison is made between our results, and previous ones derived based on the semi-classical generalized Wiener–Khintchine formula.

PACS numbers: 82.37.-j, 05.10.Gg, 33.80.-b, 42.50.Ar

I. INTRODUCTION

Physical, Chemical, and Biological systems are investigated in many laboratories using single molecule spectroscopy [1]. The investigation of the distribution of the number of photons emitted from a single molecule source is the topic of extensive theoretical research e.g. [2, 3, 4, 5, 6, 7, 8, 9, 10, 11, 12, 13, 14] and [15] for a review. Since optical properties of single molecules are usually very sensitive to dynamics and statics of their environment, and since the technique removes the many particle averaging found in conventional measurement techniques, single molecule spectroscopy reveals interesting fluctuation phenomena. An important mechanism responsible for the fluctuations in the number of photons emitted from a single molecule source is spectral diffusion e.g. [16, 17, 18, 19, 20]. In many cases the absorption frequency of the molecule will randomly change due to different types of interactions between the molecule and its environment (e.g. [15, 21, 22, 23, 24, 25, 26] and Ref. therein). For example for single molecules embedded in low temperature glasses, flipping two level systems embedded in the glassy environment, induce stochastic spectral jumps in the absorption frequency of the single molecule under investigation [19, 22, 27]. In this way the molecule may come in and out of resonance with the continuous wave laser field with which it is interacting.

Obviously a second mechanism responsible for fluctuations of photon counts is the quantum behavior of the spontaneous emission process [28, 30]. In his fundamental work Mandel [31] showed that a single atom in the process of resonance fluorescence, *in the absence of spectral diffusion*, exhibits sub-Poissonian photon statistics [32]. Photon statistics is characterized by Mandel's Q parameter

$$Q = \frac{\overline{N^2} - \overline{N}^2}{\overline{N}} - 1 \tag{1}$$

where N is the number of emitted photons within a certain time interval. The case $Q < 0$ is called sub-Poissonian behavior, while $Q > 0$ is called super-Poissonian. Sub-Poissonian statistics has no classical analog [31]. Briefly, the effect is related to anti-bunching of photons emitted from a single source and to Rabi-oscillations of the excited state population which favors an emission process with some periodicity in time (see details below). Sub-Poissonian photon statistics and photon anti-bunching were measured in several single molecule, and single quantum dots experiments [33, 34, 35, 36, 37, 38, 39]. While sub-Poissonian statistics is well understood in the context of resonance fluorescence of an isolated electronic transition of a simple atom in the gas phase, our theoretical understanding of sub-Poissonian statistics for a molecule embedded in a fluctuating condensed phase environment is still in its infant stages.

In this paper we obtain an exact analytical expression for the Q parameter in the long time limit, for a single molecule undergoing a stochastic spectral diffusion process. To obtain the exact solution we use the Zheng-Brown generating function method for single molecule photon statistics [40, 41, 42]. For the spectral diffusion we use a simple stochastic approach, in the spirit of the Kubo–Andersen line shape theory [43, 44]. The model exhibits generic behaviors of line shapes of molecules embedded in a condensed phase environment, e.g. motional narrowing when the stochastic fluctuations are fast, power broadening etc. We show that the Q parameter exhibits rich types of behaviors, in particular

it reveals the quantum nature of the emission process in the sub-Poissonian regime, while the corresponding model line-shape exhibits a classical behavior. A brief summary of our results was recently published [45].

Our analytical expressions for Q classify the transitions between sub and super Poissonian statistics. They give the conditions on the spectral diffusion time scale for sub-Poissonian behavior. Motional narrowing type of effect is revealed also for the Q parameter. Our exact result is valid for weak and strong excitation (i.e arbitrary Rabi frequency). It yields the lower bound on Q. The solution shows how we may choose the Rabi frequency so that the quantum nature of the photon emission process becomes larger, namely how to minimize Q in the Sub-Poissonian regime. This is important for the efficient detection of quantum effects in single molecule spectroscopy, since choosing too small or too large values of the Rabi frequency results in very small and hence undetectable values of Q.

Finally our exact result is used to test the domain of validity of the generalized Wiener Khintchine which yields Q in terms of a Fourier transform of a three time dipole correlation (as well known the Wiener Khintchine theorem yields the line shape in terms of a one time dipole correlation function). The theorem [25, 26] is based on the semi-classical theory of interaction of light with matter, and on linear response theory (i.e., weak Rabi frequency), it yields $Q > 0$. As pointed out in [15, 26, 41] such a behavior is expected to be valid only for slow enough spectral diffusion processes.

II. INTRODUCTION TO SUB-POISSONIAN STATISTICS

We briefly explain some of the main ideas of sub-Poissonian statistics. The general idea is that the photons emitted from a single particle, e.g. a molecule, a nano-crystal or atom are correlated in time. Consider first a hypothetical molecule, interacting with an exciting laser field, which emits photons with a constant time interval τ between successive emission events. Then $\overline{N} = t/\tau$, $\overline{N^2} = \overline{N}^2$, and hence $Q = -1$. Due to quantum uncertainty the photon emission process is always random and therefore $-1 < Q$. Sub-Poissonian behavior where $-1 < Q < 0$ implies that the stream of photons emitted from a single source maintain correlations in their arrival times to a detector.

Usually when many molecules interact with a continuous wave laser the emission events are not correlated, and the fluorescence exhibits Poissonian statistics $Q = 0$. In contrast a single molecule, once it emits a photon, is collapsed to its ground state. Hence immediately after an emission event the molecule cannot emit a second time (it has to be re-excited by the laser). Hence successive photons emitted from a single molecule, seem to repel each other on the time axis, a non-Poissonian behavior. This well known effect is called anti-bunching [46, 47] which is related to sub-Poissonian statistics.

A second effect related to sub-Poissonian behavior are Rabi-oscillations. Consider a simple atom in the process of resonance fluorescence. When the electronic transition (frequency ω_0) is in resonance with a continuous wave laser field (frequency ω_L) the electronic transition can be approximated by a two level system. First let us mentally switch off the spontaneous emission, i.e. set the inverse life time of the transition $\Gamma = 0$. For zero detuning $\omega_L = \omega_0$ the transition will exhibit well known Rabi oscillations: the population of the excited state will behave like $\rho_{ee} = \sin^2(\Omega t/2)$. Since the population in the excited state attains its maximum (minimum) periodically, also the emission times of successive photons maintain certain degree of periodicity in time, which implies sub-Poissonian statistics. Mandel showed [31], that for a two level atom in the process of resonance fluorescence

$$Q = -\frac{6\Omega^2\Gamma^2}{\left(\Gamma^2 + 2\Omega^2\right)^2}. \tag{2}$$

When $\Omega \ll \Gamma$ we have $Q \to 0$ since then successive photon emission times are not correlated, because the time between successive emissions becomes very large. While when $\Omega \gg \Gamma$ the excited state is populated swiftly, and only the finite spontaneous emission rate delays the emission, hence $Q \to 0$ also in this case. Using Eq. (2) the lower bound $Q \geq -3/4$ is easily obtained, and the minimum $Q_{\min} = -3/4$ is obtained when $\Omega_{\min} = \Gamma/\sqrt{2}$.

III. MODEL AND GENERATING FUNCTION FORMALISM

Let N be the random number of photons emitted by a single molecule source in a time interval $(0, t)$, and $P_N(t)$ is the probability of N emission events. The information about the photon statistics is contained in the moment generating function [40]

$$2\mathcal{Y}(s) \equiv \sum_{N=0}^{\infty} s^N P_N(t) \tag{3}$$

which yields the moments of N

$$\overline{N(t)} = 2\mathcal{Y}'(1) \qquad \overline{N^2(t)} = 2\mathcal{Y}''(1) + 2\mathcal{Y}'(1), \tag{4}$$

with which the Q parameter can in principle be obtained. In Eq. (4), and in what follows, we use the notation

$$\frac{\partial}{\partial s} g(s)|_{s=1} \equiv g'(1) \tag{5}$$

and similarly for second order derivatives with respect to s. The over-line in Eq. (4) describes an average over the process of photon emission, later we will consider a second type of average with respect to the spectral diffusion process, which we will denote with $\langle ... \rangle$.

The equations of motion for the generating function was given in [40] and are called generalized optical Bloch

equation. For a chromophore with single excited and ground states, and interacting with a continuous wave laser field

$$\begin{array}{l}\dot{\mathcal{U}}(s)=-\frac{\Gamma}{2}\mathcal{U}(s)+\delta_L(t)\mathcal{V}(s)\\ \dot{\mathcal{V}}(s)=-\delta_L(t)\mathcal{U}(s)-\frac{\Gamma}{2}\mathcal{V}(s)-\Omega\mathcal{W}(s)\\ \dot{\mathcal{W}}(s)=\Omega\mathcal{V}(s)-\frac{\Gamma}{2}(1+s)\mathcal{W}(s)-\frac{\Gamma}{2}(1+s)\mathcal{Y}(s)\\ \dot{\mathcal{Y}}(s)=-\frac{\Gamma}{2}(1-s)\mathcal{W}(s)-\frac{\Gamma}{2}(1-s)\mathcal{Y}(s).\end{array} \tag{6}$$

These equations are exact within the rotating wave approximation and optical Bloch equation formalism. They yield the same type of information on photon statistics contained in the quantum jump approach to quantum optics which is used in quantum Monte Carlo simulations [30, 48]. In Eq. (6) Γ is the spontaneous emission rate of the electronic transition and Ω is the Rabi frequency. The time evolving detuning is

$$\delta_L(t)=\omega_L-\omega_0-\Delta\omega(t), \tag{7}$$

where ω_L (ω_0) is the laser frequency (the molecule's bare frequency), and $\Delta\omega(t)$ is the stochastic spectral diffusion process. In Eq. (6) it is assumed that the molecule in its excited and ground state have no permanent dipole moments, hence the system is described only by the transition dipole moment via the Rabi frequency.

The physical meaning of $\mathcal{U}(s)$, $\mathcal{V}(s)$, and $\mathcal{W}(s)$ and their relation to the standard Bloch equation was given in [40], some discussion on this issue will follow Eq. (10). For related work on the foundations of these equations see [49, 50] and Ref. therein. Note that when $s\to 1$ the damping terms in Eq. (6) become small [i.e. the $(1-s)\Gamma/2$ terms], hence relaxation of the generalized Bloch equations in the important limit of $s\to 1$ is slow.

In what follows we will consider the moments $\overline{N(t)}$, $\overline{N^2(t)}$. For this aim it is useful to derive equations of motion for the vector $z=$

$$\{\mathcal{U}(1),\mathcal{V}(1),\mathcal{W}(1),\mathcal{Y}(1),\mathcal{U}'(1),\mathcal{V}'(1),\mathcal{W}'(1),\mathcal{Y}'(1),\mathcal{Y}''(1)\}. \tag{8}$$

Taking the first and the second derivative of Eq. (6) with respect to s and setting $s=1$, we find

$$\dot{z}=M(t)z \tag{9}$$

where $M(t)$ is a 9×9 matrix $M(t)=$

$$\begin{pmatrix} -\frac{\Gamma}{2} & \delta_L(t) & 0 & 0 & 0 & 0 & 0 & 0 & 0\\ -\delta_L(t) & -\frac{\Gamma}{2} & -\Omega & 0 & 0 & 0 & 0 & 0 & 0\\ 0 & \Omega & -\Gamma & -\Gamma & 0 & 0 & 0 & 0 & 0\\ 0 & 0 & 0 & 0 & 0 & 0 & 0 & 0 & 0\\ 0 & 0 & 0 & 0 & -\frac{\Gamma}{2} & \delta_L(t) & 0 & 0 & 0\\ 0 & 0 & 0 & 0 & -\delta_L(t) & -\frac{\Gamma}{2} & -\Omega & 0 & 0\\ 0 & 0 & -\frac{\Gamma}{2} & -\frac{\Gamma}{2} & 0 & \Omega & -\Gamma & -\Gamma & 0\\ 0 & 0 & \frac{\Gamma}{2} & \frac{\Gamma}{2} & 0 & 0 & 0 & 0 & 0\\ 0 & 0 & 0 & 0 & 0 & 0 & \Gamma & \Gamma & 0 \end{pmatrix} \tag{10}$$

The first three lines of $M(t)$ describe the evolution of $\mathcal{U}(1),\mathcal{V}(1),\mathcal{W}(1)$, these are the standard optical Bloch equations in the rotating wave approximation [28]. These equations yield $\mathcal{W}(1)$ which in turn gives the mean number of photons using Eq. (4)

$$\dot{\overline{N}}(t)=\Gamma\left[\mathcal{W}(1)+\frac{1}{2}\right], \tag{11}$$

and us-usual $\mathcal{W}(1)+\frac{1}{2}$ is the population in the excited state. The fourth line of $M(t)$ is zero, it yields $\dot{\mathcal{Y}}(1)=0$, this equation describes the normalization condition of the problem namely $\mathcal{Y}(1)=1/2$ for all times t [to see this use Eq. (3) and $\sum_{N=0}^{\infty}P_N(t)=1$]. The evolution of the other terms $\mathcal{U}'(1),\mathcal{V}'(1),\mathcal{W}'(1),\mathcal{Y}''(1)$ are of current interest since they describe the fluctuation of the photon emission process. In particular using Eqs. (4,10)

$$\frac{\mathrm{d}}{\mathrm{d}t}\overline{N(t)[N(t)-1]}=\Gamma\left[\overline{N(t)}+2\mathcal{W}'(1)\right]. \tag{12}$$

Solutions of time dependent equations like Eq. (9) are generally difficult to obtain, a formal solution is given in terms of the time ordering operator T, $z(t)=T\exp[\int_0^t M(t)\mathrm{d}t]z(0)$.

Eq. (9) yields a general method for the calculation of Q for a single molecule undergoing a spectral diffusion process. The aim of this paper is to obtain an exact solution of the problem for an important stochastic process used by Kubo and Anderson [43, 53, 54] to investigate characteristic behaviors of line shapes. We assume $\Delta\omega(t)=\nu h(t)$ where ν describe frequency shifts, and $h(t)$ describes a random telegraph process: $h(t)=1$ or $h(t)=-1$. The transition rate between state up (+) and state down (-) and vice versa is R. This dichotomic process is sometimes called the Kubo-Anderson process [56]. It was used to describe generic behaviors of line shapes [22, 26, 55, 56], here our aim is to calculate Q describing the line shape fluctuations.

We use Burshtein's method [51, 52] of marginal averages, to solve the stochastic differential matrix equation (9). The method yields the average $\langle z\rangle$ with respect to the stochastic process. We will calculate $\langle z\rangle$ in the limit of long times, and then obtain the steady state behavior of the line shape

$$I(\omega_L)=\lim_{t\to\infty}\frac{\mathrm{d}}{\mathrm{d}t}\langle\overline{N}(t)\rangle \tag{13}$$

and the Q parameter. Let $\langle z\rangle_{\pm}$ be the average of $z(t)$ under the condition that at time t the value of $h(t)=\pm 1$ respectively. $\langle z\rangle_{\pm}$ are called marginal averages, the complete average is $\langle z\rangle=\langle z\rangle_{+}+\langle z\rangle_{-}$. The equation of motion for the marginal averages is an 18×18 matrix equation

$$\begin{pmatrix}\langle\dot{z}_{+}\rangle\\ \langle\dot{z}_{-}\rangle\end{pmatrix}=\begin{pmatrix}M_{+}-RI & RI\\ RI & M_{-}-RI\end{pmatrix}\begin{pmatrix}\langle z_{+}\rangle\\ \langle z_{-}\rangle\end{pmatrix}. \tag{14}$$

In Eq. (14) the matrix $M_{\pm}$ is identical to matrix M in Eq. (10) when $\delta_L(t)$ is replaced by $\delta_L^{\pm}=\omega_L-\omega_0\mp\nu$, and I is a 9×9 identity matrix. In the next subsection

we obtain the long time solution of Eq. (14), the reader not interested in the mathematical details may skip to subsection IV A, where the solution for the line shape and Q is presented.

IV. MATHEMATICAL DERIVATION OF EXACT SOLUTION

In three main steps, we now find the long time behavior of the marginal averages, with which the line and Q are then obtained.

1. As mentioned, from normalization condition we have $\mathcal{Y}(1) = 1/2$ for all times. Eq. (14) yields the marginal averages $\langle\mathcal{Y}(1)\rangle_+ = \langle\mathcal{Y}(1)\rangle_- = 1/4$, in the steady state. Inserting these identities in Eq. (14) we obtain an equation of motion for the vector

$$y \equiv \langle\{\mathcal{U}(1)_+, \mathcal{V}(1)_+, \mathcal{W}(1)_+, \mathcal{U}(1)_-, \mathcal{V}(1)_-, \mathcal{W}(1)_-\}\rangle \tag{15}$$

$$\dot{y} = Ay + b_0 \tag{16}$$

where $A =$

$$\begin{pmatrix} -\frac{\Gamma}{2}-R & \delta_L^+ & 0 & R & 0 & 0 \\ -\delta_L^+ & -\frac{\Gamma}{2}-R & -\Omega & 0 & R & 0 \\ 0 & \Omega & -\Gamma-R & 0 & 0 & R \\ R & 0 & 0 & -\frac{\Gamma}{2}-R & \delta_L^- & 0 \\ 0 & R & 0 & -\delta_L^- & -\frac{\Gamma}{2}-R & -\Omega \\ 0 & 0 & R & 0 & \Omega & -\Gamma-R \end{pmatrix} \tag{17}$$

and $b_0 = (0, 0, -\Gamma/4, 0, 0, -\Gamma/4)$. In the long time limit the solution of Eq. (16) reaches a steady state (ss) given by

$$y^{ss} = -A^{-1}b_0, \tag{18}$$

and A^{-1} is the inverse of A. From Eq. (18) we find

$$\langle\mathcal{W}^{ss}(1)\rangle_+ = \frac{\Gamma}{4}\left(A_{33}^{-1} + A_{36}^{-1}\right),$$

$$\langle\mathcal{W}^{ss}(1)\rangle_- = \frac{\Gamma}{4}\left(A_{63}^{-1} + A_{66}^{-1}\right), \tag{19}$$

where $A_{36}^{-1} = A_{63}^{-1}$, and A_{ij}^{-1} is the ij matrix element of A^{-1}, $i, j = 1, \cdots, 6$. We note that $\langle\mathcal{W}^{ss}(1)\rangle_\pm$ yields the steady state marginal averages of the population difference between the excited and ground state. From Eq. (4) we see that we need $2\langle\mathcal{Y}'(1)\rangle$ to obtain the average number of photon emissions $\langle\overline{N}\rangle$. We use Eq. (14) and show

$$\langle\mathcal{Y}'^{\,ss}(1)\rangle = \langle\mathcal{Y}'^{\,ss}(1)\rangle_+ + \langle\mathcal{Y}'^{\,ss}(1)\rangle_- =$$

$$\frac{\Gamma}{2}\left(\langle\mathcal{W}^{ss}(1)\rangle_+ + \langle\mathcal{W}^{ss}(1)\rangle_- + \frac{1}{2}\right)t \tag{20}$$

and

$$\langle\mathcal{Y}'^{\,ss}(1)\rangle_+ - \langle\mathcal{Y}'^{\,ss}(1)\rangle_- = \frac{\Gamma\left(\langle\mathcal{W}^{ss}(1)\rangle_+ - \langle\mathcal{W}^{ss}(1)\rangle_-\right)}{4R}. \tag{21}$$

The average number of emitted photon, in the long time limit is (4, 20)

$$\langle\overline{N}\rangle = \Gamma\left(\langle\mathcal{W}^{ss}(1)\rangle_+ + \langle\mathcal{W}^{ss}(1)\rangle_- + \frac{1}{2}\right)t, \tag{22}$$

namely $\langle\overline{N}\rangle$ is proportional to the steady state occupation in the excited state. The line shape is

$$I(\omega_L) = \frac{I_+ + I_-}{2} \tag{23}$$

where

$$I_\pm = 2\Gamma\left[\langle\mathcal{W}^{ss}(1)\rangle_\pm + \frac{1}{4}\right]. \tag{24}$$

2. We use the solutions obtained in previous step to obtain inhomogeneous equations for $x = \langle\{\mathcal{U}'(1)_+, \mathcal{V}'(1)_+, \mathcal{W}'(1)_+, \mathcal{U}'(1)_-, \mathcal{V}'(1)_-, \mathcal{W}'(1)_-\}\rangle$,

$$\dot{x} = Ax + b(t) \tag{25}$$

where and $b(t) = (0, 0, b_+(t), 0, 0, b_-(t))$ with

$$b_\pm(t) = -\frac{\Gamma}{8} - \frac{\Gamma}{2}\langle\mathcal{W}^{ss}(1)\rangle_\pm - \frac{\Gamma^2 t}{8}\left\{1 + 2\left[\langle\mathcal{W}^{ss}(1)\rangle_+ + \langle\mathcal{W}^{ss}(1)\rangle_-\right]\right\} \pm \frac{\Gamma^2}{8R}\left[\langle\mathcal{W}^{ss}(1)\rangle_- - \langle\mathcal{W}^{ss}(1)\rangle_+\right]. \tag{26}$$

In the long time limit we obtain

$$x(t) \sim A^{-1}c_0 + \left(A^{-1}t + A^{-1}A^{-1}\right)c_1 \tag{27}$$

where c_0 and c_1 are column vectors

$$c_0 = (0, 0, c_+, 0, 0, c_-), \quad c_1 = \left(0, 0, \frac{\Gamma I(\omega_L)}{4}, 0, 0, \frac{\Gamma I(\omega_L)}{4}\right), \tag{28}$$

with

$$c_{\pm}=\frac{\Gamma}{2}\left[\langle\mathcal{W}^{ss}\left(1\right)\rangle_{\pm}+\frac{1}{4}\right]\mp\frac{\Gamma^{2}}{8R}\left[\langle\mathcal{W}^{ss}\left(1\right)\rangle_{-}-\langle\mathcal{W}^{ss}\left(1\right)\rangle_{+}\right] \tag{29}$$

we therefore obtain

$$\langle\mathcal{W}'^{\ ss}\left(1\right)\rangle_{+}=A_{33}^{-1}c_{+}+A_{36}^{-1}c_{-}+I(\omega_{L})\langle\mathcal{W}^{ss}\left(1\right)\rangle_{+}t+\frac{\Gamma I\left(\omega_{L}\right)}{4}\left[\left(A^{-1}A^{-1}\right)_{33}+\left(A^{-1}A^{-1}\right)_{36}\right] \tag{30}$$

$$\langle\mathcal{W}'^{\ ss}\left(1\right)\rangle_{-}=A_{63}^{-1}c_{+}+A_{66}^{-1}c_{-}+I(\omega_{L})\langle\mathcal{W}^{ss}\left(1\right)\rangle_{-}t+\frac{\Gamma I\left(\omega_{L}\right)}{4}\left[\left(A^{-1}A^{-1}\right)_{63}+\left(A^{-1}A^{-1}\right)_{66}\right]. \tag{31}$$

3. From Eq. (4), $\langle\overline{N^{2}(t)}\rangle=\langle2\mathcal{Y}''(1)\rangle+\langle2\mathcal{Y}'(1)\rangle$. In steady state we have

$$\langle\mathcal{Y}''^{ss}\left(1\right)\rangle=\langle\mathcal{Y}''^{ss}\left(1\right)\rangle_{+}+\langle\mathcal{Y}''^{ss}\left(1\right)\rangle_{-}. \tag{32}$$

From Eq. (14) one can show that in the long time limit

$$\langle\mathcal{Y}''^{\ ss}(1)\rangle\sim4\left[\langle\mathcal{W}^{ss}(1)\rangle_{+}c_{+}+\langle\mathcal{W}^{ss}(1)\rangle_{-}c_{-}\right]t+$$

$$+\frac{\Gamma^{2}I(\omega_{L})}{4}\left[\left(A^{-1}A^{-1}\right)_{33}+\left(A^{-1}A^{-1}\right)_{36}+\left(A^{-1}A^{-1}\right)_{63}+\left(A^{-1}A^{-1}\right)_{66}\right]t$$

$$+\frac{\Gamma I\left(\omega_{L}\right)}{2}\left[\langle\mathcal{W}^{ss}(1)\rangle_{+}+\langle\mathcal{W}^{ss}(1)\rangle_{-}+\frac{1}{2}\right]t^{2}. \tag{33}$$

Finally we obtain the Q parameter using:

$$Q=\frac{\langle\mathcal{Y}''(1)^{\mathrm{ss}}\rangle-2\langle\mathcal{Y}'(1)^{\mathrm{ss}}\rangle^{2}}{\langle\mathcal{Y}'(1)^{\mathrm{ss}}\rangle}. \tag{34}$$

Using Eqs. (20,33,34) we obtain the main result of this manuscript

$$Q=\frac{\Gamma^{2}}{2}\sum_{i=3,6}\sum_{j=3,6}\left(A^{-1}A^{-1}\right)_{ij}+\frac{\Gamma^{2}}{RI(\omega_{L})}\left[\langle\mathcal{W}^{ss}(1)\rangle_{+}-\langle\mathcal{W}^{ss}(1)\rangle_{-}\right]^{2}+\frac{\Gamma}{I\left(\omega_{L}\right)}\sum_{k=\pm}\left\{\langle\mathcal{W}^{ss}(1)\rangle_{k}\left[1+4\langle\mathcal{W}^{ss}(1)\rangle_{k}\right]\right\}, \tag{35}$$

which is valid when measurement time $t\to\infty$. The Q parameter in Eq. (35) is expressed in terms of A^{-1}. To obtain the solution in terms of the original parameters of the problem $R,\nu,\omega_{L},\omega_{0},\Omega,\Gamma$, we found analytical expressions for A^{-1} using Mathematica. The formula for the Q parameter is given in the following subsection.

A. Exact Solution

Without loss of generality we set $\omega_0=0$, hence ω_L is the detuning. We find

$$Q=\frac{\mathrm{Numerator}\left[Q\right]}{\mathrm{Denominator}\left[Q\right]}, \tag{36}$$

$$\mathrm{Numerator}\left[Q\right]=$$

$$-2\Gamma\Omega^{2}(R(\Gamma+4R)(3\Gamma^{3}-4\Gamma\nu^{2}+24\Gamma^{2}R+16\nu^{2}R+48\Gamma R^{2})(\Gamma^{3}+6\Gamma^{2}R+8\nu^{2}R+2\Gamma(2\nu^{2}+\Omega^{2}+4R^{2}))^{3}+8(4\Gamma^{11}R-4\Gamma^{10}(\nu^{2}-21R^{2})-3072\Gamma\nu^{4}R^{5}(4\nu^{2}-\Omega^{2}-16R^{2})-4096\nu^{4}R^{6}(2\nu^{2}-\Omega^{2}-4R^{2})+15\Gamma^{9}R(\Omega^{2}+48R^{2})-8\Gamma^{8}(4\nu^{4}-27\Omega^{2}R^{2}-392R^{4}+2\nu^{2}(\Omega^{2}-48R^{2}))-4\Gamma^{5}R(128\nu^{6}+\Omega^{6}+48\Omega^{4}R^{2}+1344\Omega^{2}R^{4}+6400R^{6}+12\nu^{4}(11\Omega^{2}-272R^{2})+4\nu^{2}(9\Omega^{4}-302\Omega^{2}R^{2}-5072R^{4}))-64\Gamma^{3}R^{3}(48\nu^{6}+3\nu^{4}(11\Omega^{2}-448R^{2})+3(\Omega^{2}+4R^{2})^{2}(\Omega^{2}+16R^{2})+2\nu^{2}(5\Omega^{4}-80\Omega^{2}R^{2}-544R^{4}))-256\Gamma^{2}R^{4}(28\nu^{6}+\nu^{4}(3\Omega^{2}-332R^{2})+(\Omega^{2}+4R^{2})^{3}+2\nu^{2}(\Omega^{4}-4\Omega^{2}R^{2}-32R^{4}))+4\Gamma^{7}R(-48\nu^{4}-2\nu^{2}(9\Omega^{2}-952R^{2})+3(\Omega^{4}+89\Omega^{2}R^{2}+544R^{4}))-8\Gamma^{6}(8\nu^{6}+8\nu^{4}(\Omega^{2}-17R^{2})+2\nu^{2}(\Omega^{4}-38\Omega^{2}R^{2}-2116R^{4})-3(3\Omega^{4}R^{2}+58\Omega^{2}R^{4}+40R^{6}))-16\Gamma^{4}R^{2}(96\nu^{6}+96\nu^{4}(\Omega^{2}-31R^{2})+\nu^{2}(26\Omega^{4}-720\Omega^{2}R^{2}-6656R^{4})+3(\Omega^{6}+44\Omega^{4}R^{2}+448\Omega^{2}R^{4}+1152R^{6})))\omega_{L}^{2}+32(\Gamma+2R)(3\Gamma^{8}R+512\Gamma\nu^{4}R^{4}+512\nu^{4}R^{5}-8\Gamma^{7}(\nu^{2}-3R^{2})+\Gamma^{6}(-32\nu^{2}R+3R(\Omega^{2}-4R^{2}))-32\Gamma^{2}R^{3}(-14\nu^{4}+6\nu^{2}\Omega^{2}+3(\Omega^{2}+4R^{2})^{2})+2\Gamma^{5}(16\nu^{4}-8\nu^{2}(\Omega^{2}-3R^{2})-3R^{2}(5\Omega^{2}+104R^{2}))-8\Gamma^{3}R^{2}(-56\nu^{4}+\nu^{2}(29\Omega^{2}-40R^{2})+6(\Omega^{4}+20\Omega^{2}R^{2}+64R^{4}))-2\Gamma^{4}R(-104\nu^{4}+10\nu^{2}(5\Omega^{2}-16R^{2})+$$

$3(\Omega^4+60\Omega^2R^2+368R^4)))\omega_L^4-128\Gamma^2(\Gamma+2R)^2(4\Gamma^2(\nu^2+3R^2)+\Gamma R(16\nu^2+3\Omega^2+48R^2)+4R^2(4\nu^2+3(\Omega^2+4R^2)))\omega_L^6-256\Gamma^2R(\Gamma+2R)^3\omega_L^8)$

$$\text{Denominator}\,[Q]=$$

$R((\Gamma+4R)(\Gamma^3+6\Gamma^2R+8\nu^2R+2\Gamma(2\nu^2+\Omega^2+4R^2))+4\Gamma(\Gamma+2R)\omega_L^2)(\Gamma^6+10\Gamma^5R+64\nu^2\Omega^2R^2+4\Gamma^4(2\nu^2+\Omega^2+8R^2)+4\Gamma^3R(12\nu^2+7\Omega^2+8R^2)+16\Gamma R(2\nu^4+3\nu^2\Omega^2+\Omega^4+4\Omega^2R^2)+4\Gamma^2(4\nu^4+\Omega^4+16\Omega^2R^2+4\nu^2(\Omega^2+4R^2))+8\Gamma(\Gamma^3+6\Gamma^2R-8\nu^2R+6\Omega^2R+16R^3+2\Gamma(-2\nu^2+\Omega^2+8R^2))\omega_L^2+16\Gamma(\Gamma+2R)\omega_L^4)^2$.
The line shape is

$$I(\omega_L)=\frac{\text{Numerator}[I(\omega_L)]}{\text{Denominator}[I(\omega_L)]},\tag{37}$$

$$\text{Numerator}\,[I(\omega_L)]=$$

$\Gamma\Omega^2((\Gamma+4R)(\Gamma^3+6\Gamma^2R+8\nu^2R+2\Gamma(2\nu^2+\Omega^2+4R^2))+4\Gamma(\Gamma+2R)\omega_L^2)$,

$$\text{Denominator}\,[I(\omega_L)]=$$

$\Gamma^6+10\Gamma^5R+64\nu^2\Omega^2R^2+4\Gamma^4(2\nu^2+\Omega^2+8R^2)+4\Gamma^3R(12\nu^2+7\Omega^2+8R^2)+16\Gamma R(2\nu^4+3\nu^2\Omega^2+\Omega^4+4\Omega^2R^2)+4\Gamma^2(4\nu^4+\Omega^4+16\Omega^2R^2+4\nu^2(\Omega^2+4R^2))+8\Gamma(\Gamma^3+6\Gamma^2R-8\nu^2R+6\Omega^2R+16R^3+2\Gamma(-2\nu^2+\Omega^2+8R^2))\omega_L^2+16\Gamma(\Gamma+2R)\omega_L^4$.

1. *Exact Solution for Zero Detuning*

When the detuning is zero we find

$$Q(\omega_L=0)=-\frac{2\Gamma\Omega^2\left[4\nu^2(-\Gamma+4R)+3\Gamma(\Gamma+4R)^2\right]}{\left[4\Gamma\nu^2+(\Gamma^2+2\Omega^2)(\Gamma+4R)\right]^2}.\tag{38}$$

Using Eq. (38) the lower bound $Q(\omega_L=0)>-3/4$ is obtained. The absolute minimum of Q, i.e. $Q=-3/4$ is found when $\nu=0,\Omega=\Gamma/\sqrt{2}$, or when $R\to\infty,\Omega=\Gamma/\sqrt{2}$. Namely the absolute minimum is found for a molecule whose absorption frequency is fixed, or for a very fast spectral modulation.

Remark: Eq. (38) indicates a transition from sub-Poissonian statistics ($Q<0$) to super-Poissonian statistics ($Q>0$) when $4\nu^2=3(\Gamma+4R)^2/(\Gamma-4R)$. If $R>\Gamma/4$, i.e. if the bath is fast compared with the radiative life time, we find sub-Poissonian behavior for all values of ν and Ω.

V. THE PHYSICAL BEHAVIORS OF THE EXACT SOLUTION IN LIMITING CASES

The Q parameter is a function of two control parameters ω_L and Ω, and three model parameters Γ,R,ν. The classification of different types of physical behaviors, based on the relative magnitude of the parameters is investigated in this section. The limiting behaviors of Q are obtained from the exact solution using Mathematica.

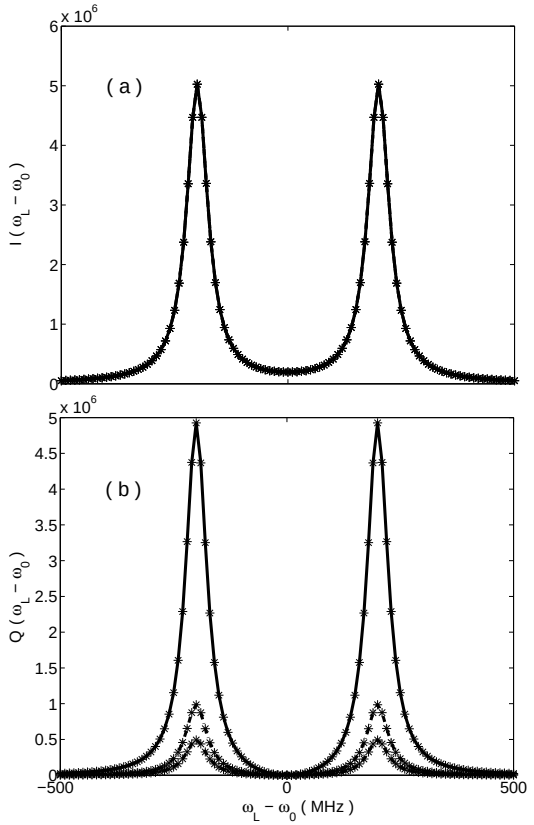

FIG. 1: The line shape $I(\omega_L-\omega_0)$ (a) and the $Q(\omega_L-\omega_0)$ parameter (b) are calculated with the exact solution Eqs. (37) and Eq. (36) respectively. In this slow modulation strong coupling limit $R<<\Gamma\simeq\Omega<<\nu$, both Q and I exhibit splitting behavior with two peaks centered at $\omega_L-\omega_0=\pm\nu$. The Q parameter exhibits super-Poissonian statistics $Q>0$. The $*$ asterisks are approximate results Eq. (39) for the line shape, and Eq. (41) for Q. Parameters are $\Gamma=40$ MHz, $\nu=5\Gamma$, $\Omega=\Gamma/\sqrt{2}$, and $R=1$ Hz (solid curve), 5 Hz (dashed-dot curve), and 25 Hz (dashed curve).

A. Slow Modulation Regime: $R<<\nu,\Gamma,\Omega$

In the slow modulation regime, the bath fluctuation process (R) is very slow compared with the radiative decay rate (Γ), frequency fluctuation amplitude (ν) and the Rabi frequency (Ω). This case is similar to situations in many single molecule experiments, for example single molecules in low temperature glasses.

The exact solution can be simplified in the limit $R\to0$, using Eq. (37)

$$\lim_{R\to0}I(\omega_L)=\frac{I_+(\omega_L)+I_-(\omega_L)}{2},\tag{39}$$

and

$$I_\pm(\omega_L)=\frac{\Gamma\Omega^2}{\left(\Gamma^2+2\Omega^2+4(\omega_L\mp\nu)^2\right)}.\tag{40}$$

The line is a sum of two Lorentzians centered on $\pm\nu$, namely it exhibits splitting behavior when $\nu >> \Gamma, \Omega$. Using Eq. (36) we find a simple super-Poissonian behavior for Q in the slow modulation limit $R \to 0$

$$Q \sim Q_{\rm slow} \equiv \frac{\left(I_+ - I_-\right)^2}{4RI}, \tag{41}$$

and since $R \to 0$, Q may become very large (e.g. $Q = 5 * 10^6$ in Fig. 1).

A simple picture can be used to understand these results. In the slow modulation limit the molecule jumps between two states + and −, the time between successive jumps is very long, in such a way that many photons are emitted between jump events. In each of these two states the molecule emits photons at a rate $I_\pm(\omega_L)$, Eq. (40). These rates are determined by the familiar steady state solutions of the optical Bloch equation, for a two level atom with the absorption frequency $\omega_0 \pm \nu$ fixed in time [28]. In this slow limit the random number of emitted photons, in time interval $(0, t)$, is $N_{\rm slow} = \int_0^t I(t)\mathrm{d}t$, and $I(t)$ is a stochastic intensity that jumps between two states $I_\pm(\omega_L)$ with the rate R. Using this simple random walk picture it is straightforward to derive Eqs. (39, 41). For mathematical details see Ref. [26] who considered a similar slow modulation limit which is valid only for weak Rabi frequency.

1. $R << \Gamma \simeq \Omega << \nu$

Within the slow modulation limit we distinguish between two cases. The case $R << \Gamma \simeq \Omega << \nu$ is called the slow modulation strong coupling limit. In this case the line and Q have two well separated peaks and the broadening of the two peaks due to the finite life time, and power of the laser field is small compared with the frequency shifts (see Fig. 1). From Fig. 1, and as expected from Eqs. (39, 41), Q decreases when R is increased, while $I(\omega_L)$ is independent of R. Thus it is Q not $I(\omega_L)$ that yields information on the dynamics. In Fig. 1 the agreement between the exact solution and the approximation Eq. (41) is good.

2. $R << \nu << \Gamma \simeq \Omega$

The limit $R << \nu << \Gamma \simeq \Omega$ is called the weak coupling slow modulation limit. In this case the two peaks of the line, discussed in the previous sub-section, are overlapping and the line is approximated by

$$I(\omega_L) \sim \frac{\Gamma\Omega^2}{\Gamma^2 + 2\Omega^2 + 4\omega_L^2}. \tag{42}$$

This result is exact when $\nu = 0$, for arbitrary R,

The behavior of Q is demonstrated in Fig. 2, where we observe both super-Poissonian and sub-Poissonian behaviors. In the slow modulation weak coupling limit, we

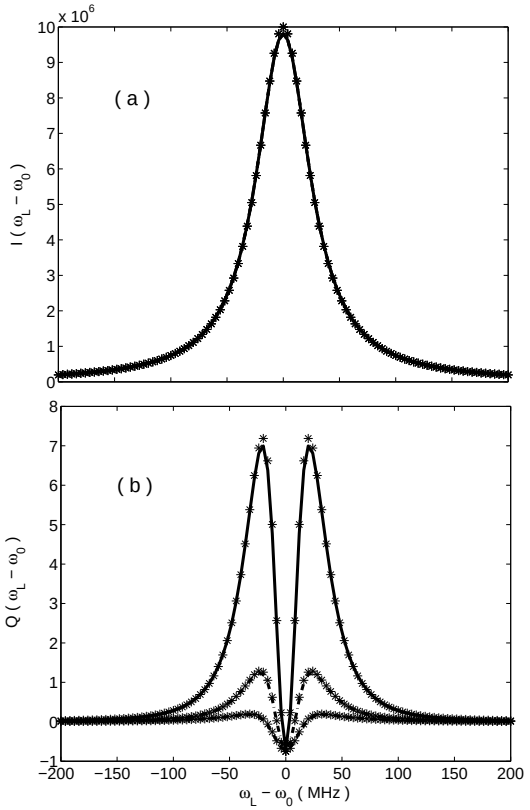

FIG. 2: Same as Fig. 1 for the slow modulation weak coupling case $R << \nu << \Gamma \simeq \Omega$. We see that the line I is Lorentzian in shape while the Q parameter exhibits splitting. And unlike the line shape Q depends on R in this limit. In the vicinity of zero detuning Q exhibits a sub-Poissonian behavior ($Q < 0$). Far from zero detuning the slow spectral diffusion process controls the behavior of Q and then $Q > 0$. The $*$ asterisk are the approximate Eqs. for Q Eq. (45) and I Eq. (42). The parameters are $\Gamma = 40$ MHz, $\nu = \Gamma/10$, $\Omega = \Gamma/\sqrt{2}$, and $R = \Gamma/2500$ (solid curve), $\Gamma/500$ (dashed-dot curve), and $\Gamma/100$ (dashed curve).

must distinguish between the cases of large and small detuning. First note that according to Eq. (41) when the detuning is zero we find $Q = 0$, namely the leading $1/R$ term in our asymptotic expansion vanishes. We must therefore consider the higher order terms in our asymptotic expansion of Eq. (36) and we find

$$Q \sim Q_{\rm slow} + Q_{\rm M} \tag{43}$$

where

$$Q_{\rm M} = -\frac{2\Omega^2\left(3\Gamma^2 - 4\omega_L^2\right)}{\left(\Gamma^2 + 2\Omega^2 + 4\omega_L^2\right)^2}. \tag{44}$$

Eq. (43) has a simple meaning, the first term is a contribution to Q from spectral diffusion, which is identical to Eq. (41). The second term $Q_{\rm M}$ is identical to the result obtained by Mandel, for the Q parameter in the absence of spectral diffusion [31], and $Q_M < 0$ provided

that the detuning is not too large. The second term is dominating over the first when the detuning is small, and for zero detuning we obtain in Eq. (43) sub-Poissonian statistics. More explicitly, we Taylor expand (40) using ν as a small parameter, and obtain for the slow modulation weak coupling limit

$$Q \simeq \frac{64\Gamma\Omega^2\omega_L^2\nu^2}{R\left(\Gamma^2+2\Omega^2+4\omega_L^2\right)^3} - \frac{2\Omega^2\left(3\Gamma^2-4\omega_L^2\right)}{\left(\Gamma^2+2\Omega^2+4\omega_L^2\right)^2}. \quad (45)$$

One may say that for zero detuning, the molecule behaves as if its absorption frequency is fixed.

To conclude, we see that in the slow modulation limit Q is a sum of two additive contributions: i) a part related to spectral diffusion $Q_{\rm slow}$ and ii) and a part related to quantum fluctuations, i.e. Q_M. Such a behavior was very recently discussed in [42] (see also [26] for related discussion). The quantum fluctuations are however bounded from above and below $-3/4 < Q_M < 0$, while the contribution from spectral diffusion is not $0 < Q_{\rm slow} < \infty$. Hence detection of the quantum fluctuations is possible only when $Q_{\rm slow}$ is small, which for our case implies zero detuning and weak coupling limit.

B. Fast Modulation Regime: $R >> \nu, \Gamma, \Omega$

We now consider the fast modulation limit. If we take $R \to \infty$ keeping Ω, Γ, and ν fixed we find from Eq. (36)

$$\lim_{R\to\infty} Q = Q_{\rm M} \quad (46)$$

given in Eq. (44). Hence in this limit we find a sub-Poissonian behavior, provided that the detuning ω_L is not too large. The line shape is identical to the expression on the right hand side of Eq. (42). This behavior is expected, when the spectral diffusion is very fast the emitting single molecule cannot respond to the stochastic fluctuations.

A more interesting case is to let $R \to \infty$ and $\nu \to \infty$ but keep,

$$\Gamma_{\rm SD} \equiv \frac{\nu^2}{R} \quad (47)$$

finite. We call this limit the fast modulation limit, using Eq. (37) the line shape is

$$I_{\rm fast}\left(\omega_L\right) = \frac{\left(\Gamma+\Gamma_{\rm SD}\right)\Omega^2}{\left(\Gamma_{\rm SD}+\Gamma\right)^2 + 2\left(1+\Gamma_{\rm SD}/\Gamma\right)\Omega^2 + 4\omega_L^2}, \quad (48)$$

and when the Rabi frequency is small

$$I_{\rm\ fast}\left(\omega_L\right) \sim \frac{\left(\Gamma+\Gamma_{\rm SD}\right)\Omega^2}{\left(\Gamma_{\rm SD}+\Gamma\right)^2+4\omega_L^2}. \quad (49)$$

In this limit we have the well known effect of motional narrowing: the width of the line is determine by $\Gamma + \Gamma_{\rm SD}$ and as the process becomes faster the line becomes narrower, namely $\Gamma_{\rm SD}$ decreases when R is increased.

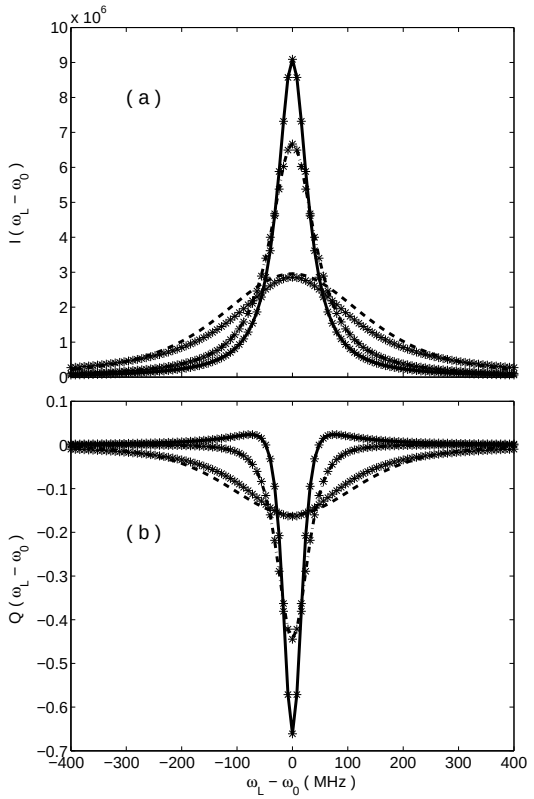

FIG. 3: Same as Fig. 1 for fast modulation $R >> \nu >> \Omega = \Gamma/\sqrt{2}$. We see quantum fluctuations namely $Q < 0$. Both for the line shape and for Q we have motional narrowing behavior, as the spectral diffusion process becomes faster Q and I narrow. When $R \to \infty$, Q approaches Mandel's formula Eq. (44). In the same limit the width of the line shape is determined only by its natural width, namely by the inverse radiative life time of the excited state (provided that the Rabi frequency is weak). The $*$ asterisk are the approximations for Q Eq. (50) and $I(\omega_L)$ Eq. (48). The parameters are $\Gamma = 40$ MHz, $\nu = 5\Gamma$, $\Omega = \Gamma/\sqrt{2}$, and $R = 5\Gamma$ (dashed curve), 25Γ (dashed-dot curve), and 125Γ (solid curve).

The Q parameter is obtained from Eq. (36)

$$Q_{\rm fast} = -\frac{2\Gamma\Omega^2\left[3\Gamma^3+5\Gamma\Gamma_{\rm SD}^2+\Gamma_{\rm SD}^3-4\Gamma\omega_L{}^2+\Gamma_{\rm SD}\left(7\Gamma^2+4\omega_L^2\right)\right]}{\left[\Gamma^3+\Gamma\Gamma_{\rm SD}{}^2+2\Gamma\Omega^2+2\Gamma_{\rm SD}\left(\Gamma^2+\Omega^2\right)+4\Gamma\omega_L^2\right]^2}. \quad (50)$$

Thus in the fast modulation limit the photon statistics is sub-Poissonian provided that the detuning is not too large. When $\Gamma_{SD} \to 0$ the result for Q reduces to Mandel's result Eq. (44). In Fig. 3, we show the line shape and the Q parameter, for three values of the jump rate (R) in the fast modulation regime while ν, Ω, Γ are kept fix. We see that as the stochastic spectral diffusion process gets faster, both the line shape and the Q parameter

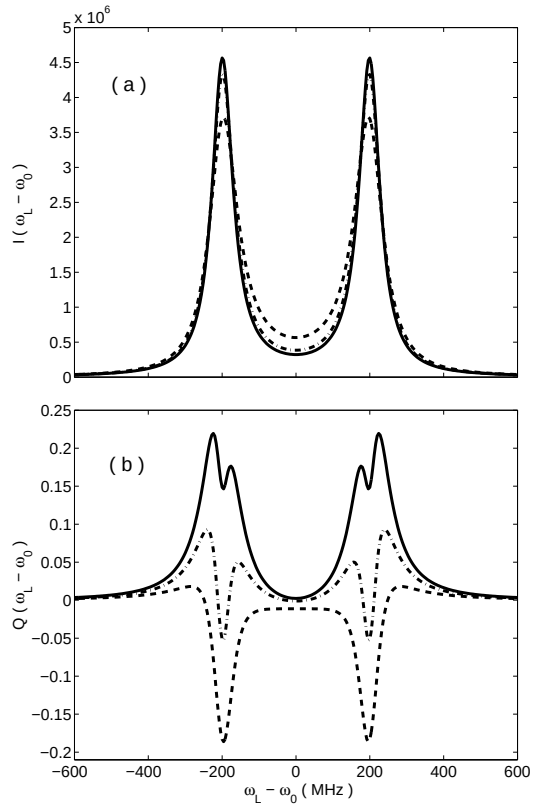

FIG. 4: We show the transition of the Q parameter from sub-Poissonian behavior, to super Poissonian behavior as the rate R is changed. Note that Q exhibits a non-trivial behavior: it may have four peaks. Such a behavior is limited to a small regime of parameters when $R \simeq \Gamma \simeq \Omega$ and was not observed in other limits of the problem. The parameters are $\Gamma = 40$ MHz, $\nu = 5\Gamma$, $\Omega = \Gamma/\sqrt{2}$, and $R = \Gamma/6$ (solid curve), $\Gamma/4$ (dashed-dot curve), and $\Gamma/2$ (dashed curve).

become narrow. Thus both $I(\omega_L)$ and Q exhibit a motional narrowing effect. Also, as the stochastic process gets faster, a stronger quantum behavior is obtained, in the sense that the minimum of Q decreases.

C. Strong coupling limit $\nu >> R, \Gamma, \Omega$

To investigate the strong coupling limit we consider the value of Q for $\omega_L = \nu$, and $\nu >> \Gamma, R, \Omega$. From Eq. (36) we obtain

$$\lim_{\nu\to\infty} Q_{\omega_L=\nu} = -\frac{(\Gamma+2R)\,\Gamma\Omega^2\left[-\Gamma^3+16\Gamma R^2+8R^3-2\Gamma\Omega^2+2R\left(2\Gamma^2+\Omega^2\right)\right]}{2R\left[\Gamma^3+4\Gamma R^2+2\Gamma\Omega^2+2R\left(2\Gamma^2+\Omega^2\right)\right]^2}. \tag{51}$$

This equation exhibits both sub-Poissonian and super–Poissonian behaviors. When the process is very *slow*, namely $R \to 0$, we obtain

$$\lim_{\nu\to\infty} Q_{\omega_L=\nu} \sim \frac{\Gamma\Omega^2}{2R\left(\Gamma^2+2\Omega^2\right)} \tag{52}$$

a super-Poissonian behavior. In the *intermediate modulation limit*, when $R = \Gamma$, we obtain

$$\lim_{\nu\to\infty} Q_{\omega_L=\nu} = -\frac{81\Omega^2\Gamma^2}{2\left(9\Gamma^2+4\Omega^2\right)^2} \tag{53}$$

a sub-Poissonian behavior. When $R \to \infty$ we find that Q is small

$$\lim_{\nu\to\infty} Q_{\omega_L=\nu} \sim -\frac{\Omega^2}{2R\Gamma}. \tag{54}$$

Eqs. (52-54) are valid only in the limit of $\nu \to \infty$. However behaviors similar to the predictions of these equations are found also for finite values of ν. On $\omega_L = \nu$ we have three typical behaviors: (*i*) $Q(\omega_L = \nu) > 0$ when the process is slow, see Fig. 1). (*ii*) $Q(\omega_L = \nu) < 0$ when $\Gamma \simeq R$, see Fig. 4 for $R = \Gamma/2$, and (*iii*) when $R \to \infty$ we find $Q\left(\omega_L = \nu\right) \to 0$, Fig. 3.

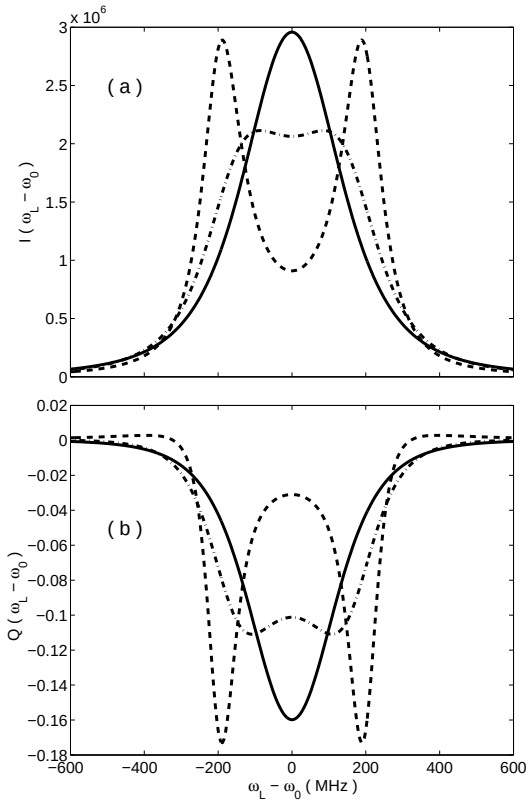

FIG. 5: Sub - Poissonian behaviors of Q for the case of strong coupling $\nu >> R$ and intermediate modulation $R \simeq \Gamma \simeq \Omega$ limit. Q exhibits two types of quantum sub-Poissonian statistics: i) splitting behavior and ii) motional narrowing behavior where Q has a single minimum. The parameters are: $\Gamma = 40$ MHz, $\nu = 5\Gamma$, $\Omega = \Gamma/\sqrt{2}$, and $R = 1\Gamma$ (dashed curve), 3Γ (dashed-dot curve), and 5Γ (solid curve).

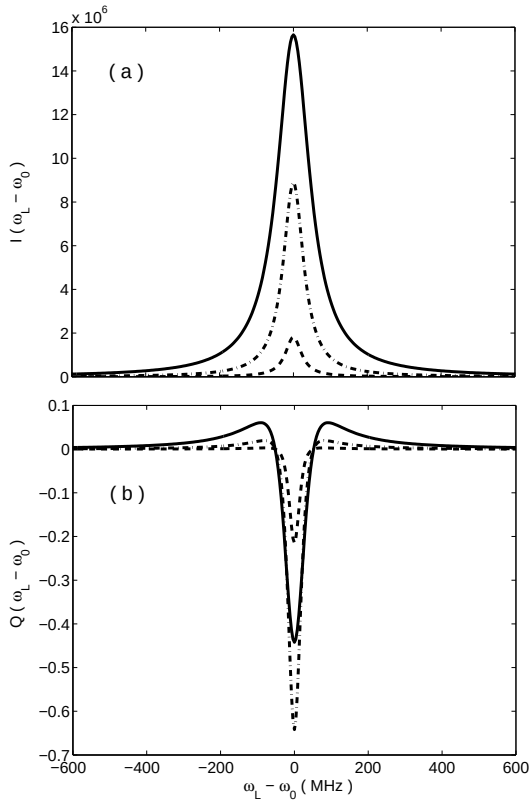

FIG. 6: We investigate the dependence the line shape and Q on the Rabi frequency Ω. Power broadening of the line is observed, while for the Q parameter we have a turn-over behavior as explained in the text. The three values of the Rabi frequency are $\Omega = \Gamma/4$ (dashed curve), $\Gamma/\sqrt{2}$ (dashed-dot curve), and $3\Gamma/2$ (solid curve). And the minimum of Q, on zero detuning, is obtained for the intermediate value of $\Omega = \Gamma/\sqrt{2}$. The fixed parameters are $\Gamma = 40$ MHz, $\nu = 5\Gamma$, and $R = 100\Gamma$.

D. Intermediate Modulation Limit $R \simeq \Gamma$

When $R \simeq \Gamma \simeq \Omega << \nu$ we obtain interesting behaviors for Q. In Fig. 4 the Q parameter shows a transition from sub-Poissonian to super Poissonian, photon statistics. In this regime of parameters, the shape of Q when plotted as a function of ω_L is very sensitive to the value of the control parameters e.g. in Fig. 4 we change R only moderately still we see very different types of behaviors for Q. For certain values of parameters Q attains more than two peaks (see Fig. 4 for $R = \Gamma/6, \Gamma/4$). In contrast $I(\omega_L)$ exhibits a simple splitting behavior with two peaks on $\pm\nu$, which is similar to the slow modulation case.

Besides the transition from sub to super Poissonian behavior, a second type of transition is observed as R is increased. In our problem we have two types of sub-Poissonian behavior. We noticed already that when the stochastic modulation becomes very fast, Q has one minimum on zero detuning (see Fig. 2), while when $R \simeq \Gamma$, Q has two minima on $\omega_L \pm \nu$ (see Fig. 3 and $R = \Gamma/2$). The transition between these two types of sub-Poissonian behaviors is shown in Fig. 5.

VI. EXTREMUM OF Q

We now investigate the dependence of Q on the excitation field. In Fig. 6 we consider an example line shape and Q parameter, where we fix the model parameters ν, R, Γ and vary the Rabi frequency. For the line we see well known power broadening: as the Rabi frequency is increased the line becomes wider, and as expected the photon emission rate $I(\omega_L)$ increases monotonically when Ω is increased. For the Q parameter we have a turn-over behavior, as we increase Ω the value of Q on zero detuning decreases then increases.

Generally this type of turn-over is expected, since as discussed in Sec. II, $Q = 0$ when $\Omega \to \infty$ or $\Omega \to 0$. Thus there exists an optimal Rabi frequency which yields an extremum of Q. Obviously it is important to obtain the values of Ω which yield the extremum of Q, since then

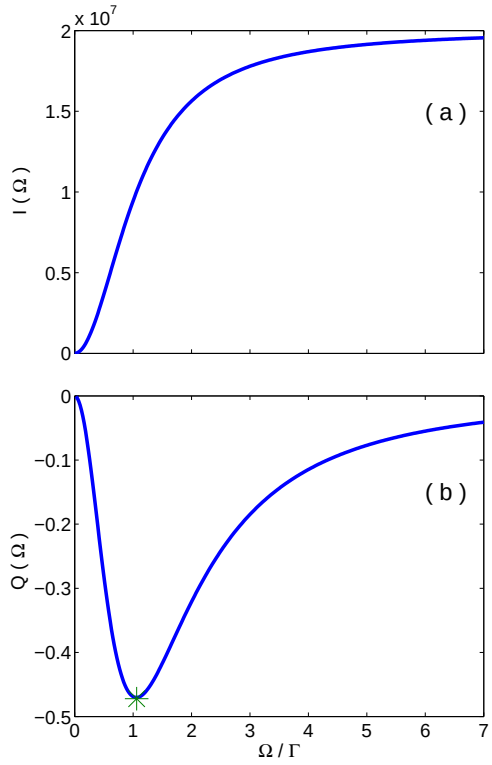

FIG. 7: The photon emission rate $I(\Omega)$ (a) the $Q(\Omega)$ parameter (b) are calculated with the exact solution of Eq. (37) and Eq. (36), in the fast modulation limit. The parameters are $\Gamma = 40$ MHz, $\nu = 5\Gamma$, $\omega_L = 0$, $\Omega = 0 \to 7\Gamma$, and $R = 10\Gamma$. We observe the saturation of the line as Ω becomes large, while $Q(\Omega)$ has a minimum. The value of Ω which minimizes $Q(\Omega)$ is of interest since it yields the strongest quantum fluctuations. The symbol $*$ is the point $(\Omega_{\min}, Q_{\min})$ calculated based on the approximation Eqs. (57,58).

the fluctuations are the largest. The extremum can be either a minimum or a maximum, as we shall show now.

A. Largest Quantum Fluctuations

We now consider the quantum regime $Q < 0$. In Fig. 7(b) we demonstrate the turn-over behavior of $Q(\Omega)$ for an example where the stochastic fluctuations are fast. In this fast modulation case $Q < 0$ hence $Q(\Omega)$ has a minimum. For the same parameters the photon emission rate $I(\Omega)$ saturates as Ω is increased, and the emission rate is never faster than Γ [see Fig. 7(a)].

Let $\Omega_{\min}$ be the Rabi frequency which minimizes Q in the sub-Poissonian case $Q < 0$, and $Q_{\min}$ the corresponding value of Q. Using Eq. (38) we find for zero detuning, and for $R > \Gamma/4$

$$\Omega_{\min} = \sqrt{\frac{\Gamma^3 + 4\Gamma^2 R + 4\Gamma\nu^2}{2\,(\Gamma + 4R)}} \tag{55}$$

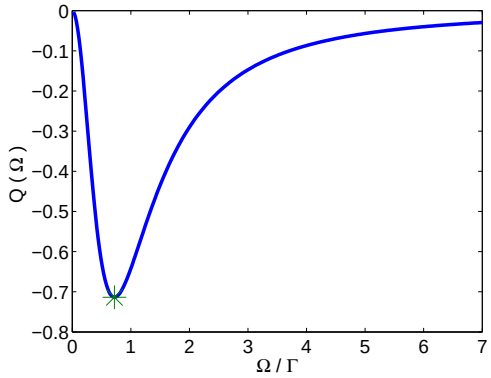

FIG. 8: We demonstrate how to choose the Rabi frequency in order to obtain strong sub-Poissonian behavior. The $Q(\Omega)$ parameter is calculated with the exact solution of Eq. (36). The detuning $\omega_L - \omega_0$ is zero, and $\Gamma = 40$ MHz, $\nu = \Gamma/10$ and $R = \Gamma/100$ corresponding to the slow modulation weak coupling limit. The minimum, the $*$ in the figure, $Q_{\min} \simeq -0.71$ is found for $\Omega_{\min} \simeq 0.72\Gamma$, which is close to the global minimum $(Q_{\min}, \Omega_{\min}) = (-3/4, \Gamma/\sqrt{2})$.

and

$$Q_{\min} = \frac{-\left(4\,\nu^2\,(-\Gamma + 4\,R) + 3\,\Gamma\,(\Gamma + 4\,R)^2\right)}{4\,(\Gamma + 4\,R)\,(\Gamma^2 + 4\,\nu^2 + 4\,\Gamma\,R)}. \tag{56}$$

Eqs. (55,56) yield $\Omega_{\min}$ and $Q_{\min}$ in terms of ν and R. Due to motional narrowing effect, for fast processes satisfying $\nu << R$, ν and R are not easily obtained from experiment, while the parameter $\Gamma_{\rm SD}$ is in principle easy to obtain from the measurement of the line width. Using Eq. (50), we find in the fast modulation limit and for zero detuning

$$\frac{\Omega_{\min}}{\Gamma} = \sqrt{\frac{1 + \Gamma_{\rm SD}/\Gamma}{2}} \tag{57}$$

$$Q_{\min} = -\frac{(\Gamma_{\rm SD} + 3\Gamma)}{4\,(\Gamma + \Gamma_{SD})} \tag{58}$$

These simple equations relate between the width of the line given in Eq. (49) and $Q_{\min}$ and $\Omega_{\min}$. From Eqs. (57,58) we see that when $\Gamma_{SD} << \Gamma$, $\Omega_{\min} = \Gamma/\sqrt{2}$ and $Q_{\min} = -3/4$. When $\Gamma_{SD} >> \Gamma$ we find $\Omega_{\min} = \sqrt{\Gamma_{SD}\Gamma/2}$ and $Q_{\min} = -1/4$.

Remark: When the detuning is not zero, we find using Eq. (50)

$$\frac{\Omega_{\min}}{\Gamma} = \sqrt{\frac{(1 + \Gamma_{\rm SD}/\Gamma)^2 + 4\omega_L^2/\Gamma^2}{2\,(1 + \Gamma_{\rm SD}/\Gamma)}}. \tag{59}$$

Similar turn-over behaviors of $Q(\Omega)$ are found also in other non fast parameter regimes. In Fig. 8 we show $Q(\Omega)$ versus Ω for the slow modulation weak coupling

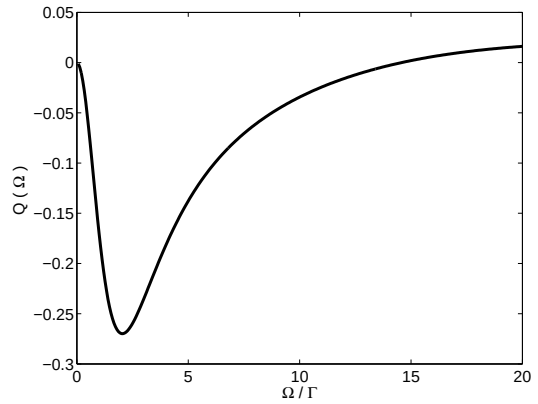

FIG. 9: Same as Fig. 8 for the intermediate modulation limit $\Gamma \simeq R$. Unlike Figs. 7,8, the detuning is on $\omega_L = \nu$. Parameters are chosen as $\Gamma = 40$ MHz, $\nu = 5\Gamma$, $\Omega = 0 \to 20\Gamma$, and $R = 2\Gamma$. The figure illustrates that the turn-over behavior of $Q(\Omega)$ is generic, and not limited to the fast modulation limits Fig. 7 and slow modulation/weak coupling limit Fig. 8.

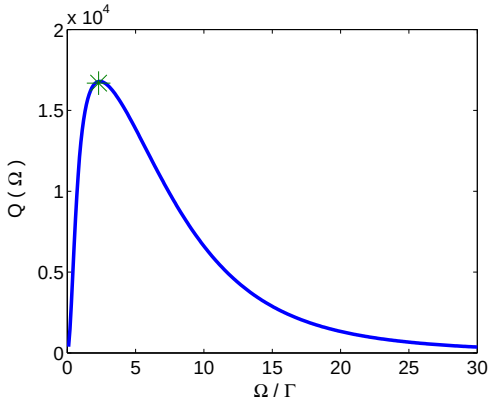

FIG. 10: The crossover behavior of the $Q(\Omega)$ parameter in the slow modulation limit. Q exhibits a super-Poissonian behavior, and $Q(\Omega)$ attains a maximum when the Rabi frequency is changed. Thus also for this classical type of behavior an extremum of the fluctuations is found for a particular value of the control parameter Ω. The parameters are $\Gamma = 40$ MHz, $\nu = 5\Gamma$, $R = 500$Hz and $\omega_L - \omega_0 = \nu$. Using the approximate Eqs. (61,62) we obtain the values $Q_{\max} \simeq 16686$ $\Omega_{\max} \simeq 2.3\Gamma$, the symbol $*$ in the figure, which is in good agreement with the exact solution (the solid curve).

limit $R < \nu < \Gamma$ and for zero detuning. Fig. 8 shows that Q exhibits a minimum as function of Ω, this minimum is found in the vicinity of $\Omega_{\min} = \Gamma/\sqrt{2}$. Such a behavior is understood based on Eq. (43), the spectral diffusion contribution for Q is not important at zero detuning, while the contribution of Q_M yields $\Omega_{\min} = \Gamma/\sqrt{2}$. To demonstrate that the turnover behavior of $Q(\Omega)$ is generic, we consider also the intermediate modulation limit in Fig. 9. Here we choose the detuning according to $\omega_L = \nu$, since the Q parameter on zero detuning is relatively small (see Fig. 5).

B. Maximum of Super-Poissonian Fluctuations

In contrast to the behaviors in the quantum regime $Q < 0$, in the slow modulation limit where $Q > 0$, $Q(\Omega)$ obtains a maximum, whose location is easy to calculate with Eq. (41). Such a behavior is demonstrated in Fig. 10 for a case when the spectral shift ν is not very large. If $\nu >> \Omega, \Gamma$ then in the slow modulation limit

$$Q_{\text{slow}} \simeq \frac{\Gamma\Omega^2}{2R\left(\Gamma^2 + 2\Omega^2\right)} - \frac{3\Gamma\Omega^2}{32R\nu^2} \tag{60}$$

when the detuning is equal to $\omega_L = \nu$. In Eq. (60) the second term on the right hand side is supposed to be a correction to the first term, namely $Q_{\text{slow}} > 0$. Let $\Omega_{\max}$ be the value of Ω which maximizes Q in the super-Poissonian regime, and $Q_{\max}$ the corresponding maximum. This maximum always exists since as mentioned $Q = 0$ when $\Omega \to 0$ or $\Omega \to \infty$. Then using Eq. (60)

$$\Omega_{\max} \simeq \sqrt{\frac{\Gamma\left(4\sqrt{3}\nu - 3\Gamma\right)}{6}} \tag{61}$$

which is independent of R and

$$Q_{\max} \simeq \frac{\Gamma\left(3\Gamma^2 + 16\nu^2 - 8\sqrt{3}\Gamma\nu\right)}{64R\nu^2}. \tag{62}$$

Note that when the frequency shifts are very large $\nu \to \infty$ we find using Eq. (61) $\Omega_{\max} \to \infty$. Hence the value of $\Omega_{\max}$ may become very large and then in experiment it is impossible to reach $\Omega_{\max}$ (e.g. $\nu = 1GHz$). If we impose the condition $\Omega << \nu$ we have

$$Q_{\text{slow}} \simeq \frac{\Gamma\Omega^2}{2R\left(\Gamma^2 + 2\Omega^2\right)} \tag{63}$$

for the laser detuning $\omega_L = \nu$. Hence Q_{slow} monotonically increases and eventually saturates, similar to the behavior of the average emission rate.

VII. SUMMARY AND DISCUSSION

The Q parameter yields informations not contained in the line shape. The most obvious is the transition from super (i.e. classical) to sub (quantum) Poissonian behavior. Such a quantum signature of the photon emission process is not obtained from the line shape. In comparison with the Q parameter of a single atomic transition, the Q parameter investigated here exhibits rich behaviors. These include splitting, both in the sub and in the super Poissonian regime, a transition from a fast to a slow modulation limit, and effects related to motional narrowing. The most non-trivial behavior is obtained in the intermediate modulation limit when $\Gamma \simeq R \simeq \Omega$ where Q attains more then two peaks.

Since Q contains the new information on single molecule experiments, namely information beyond the line shape, it is important to emphasize that Q attains an extremum for a particular value of the Rabi frequency. In particular in the sub-Poissonian regime $Q(\Omega)$ has a minimum. Hence we optimize the Rabi frequency in such a way that $|Q|$ is increased, e.g. we obtain $\Omega_{\min}$. In other words there exist an "ideal" choice of the Rabi frequency in single molecule experiments. In the quantum sub-Poissonian regime this optimal Rabi frequency cannot be considered weak, neither strong, hence perturbative approaches to single molecule spectroscopy are not likely to yield it. This is in complete contrast to most theories of line shapes which are based on the assumption of weak external fields, e.g. the Wiener–Khintchine theorem and linear response theory. Single molecule theories should be able to predict the turn-over behavior of $Q(\Omega)$ based on different models, since such a behavior is not expected to be limited to the model under investigation. Of-course the exact solution presented in this manuscript is very valuable in this direction, since it predicts precisely the details of this transition for the Kubo-Anderson stochastic process.

It would be interesting to investigate further how general are our results. From line shape theory, we know that in the fast modulation limit, line shapes have Lorentzian shapes under very general conditions. From experiment we know that motional narrowing effect, and Lorentzian behavior of lines is wide spread. Thus at-least in this limit certain general features of line shapes, which are not sensitive to model assumptions are found. Similarly, we expect, that in the fast modulation limit, some of our results are general. For example the motional narrowing behavior of Q and its approach to Mandel's behavior Q_M is likely to be general. It would be interesting to check if the relation between $Q_{\min}$ and $\Omega_{\min}$ Eq. (57,58), and the width of the line given by Γ_{SD} and Γ is valid for other models, both stochastic and Hamiltonian. These simple equations are important since they yield the optimal Rabi frequency $\Omega_{\min}$ in terms of the width of the line shape, which in turn is easily determined in usual line shape measurement.

In Ref. ([25],[26]) a semi-classical framework for the mathematical calculation of Q for single molecule spectroscopy was investigated. The approach yields the Q parameter in terms of a Fourier transform of a three time dipole correlation function. As mentioned in the introduction, the approach in ([25],[26]) is based on two main approximations (i) external fields are weak $\Omega \to 0$, i.e. linear response theory, and the (ii) semi-classical approach to photon counting statistics. The second assumption implies that $Q > 0$, and as pointed out in [15, 26] such an approach is expected to be valid for slow processes. The approach is useful since most single molecule experiments report on slow fluctuations. The results obtained in this manuscript reduce to those in ([25],[26]) in the limit of $\Omega \to 0$, and in the slow modulation limit, as they should. The quantum behavior of Q becomes important when $R \sim \Gamma$ or for faster processes. It is left for future work to construct a general quantum linear response theory, based on the Eqs. of motion 9, which would yield both super and sub-Poissonian statistics. Finally, also the investigation of the time dependence of Q is timely.

This work was supported by National Science Foundation award CHE-0344930. EB thanks the Complexity Center in Jerusalem for financial support.

[1] W. E. Moerner and M. Orrit, *Science* **283** 1670 (1999).
[2] T. Plakhotnik, *Phys. Rev. B* **59** 4658 (1999).
[3] G. K. Schenter, H. P. Lu, X. S. Xie *J. Phys. Chem. A* **103** 10477 (1999).
[4] A. M. Berezhkovskii, A. Szabo, and G. H. Weiss *J. Phys. Chem. B* **104** 3776 (2000).
[5] A. Molski et al *Chem. Phys. Lett.* **318** 352 (2000).
[6] H. Yang, X. S. Xie *J. of Chemical Physics* **117** 10965 (2002)
[7] Y. Jung, E. Barkai, and R. Silbey, *Chemical Physics* **284** 181 (2002).
[8] S. J. Jang, R. J. Silbey *J. of Chem. Phys.* **118** 9312 (2003).
[9] Z. S. Wang, D. E. Makarov *J. Phys. Chem. B* **107** 5617 (2003)
[10] R. Verberk, and M. Orrit, *J. of Chem. Phys.* **119** 2214 (2003).
[11] G. Aquino, L. Palatella, P. Grigolini *Phys. Rev. Lett.* **93** 050601 (2004).
[12] V. Barsegov, S. Mukamel *J. of Phys. Chem.* **108** 15 (2004).
[13] S. L. Yang, and J. S. Cao *J. of Chem. phys.* **121** 562 (2004).
[14] G. Margolin, E. Barkai, *J. of Chem. Phys* **121** 1566 (2004).
[15] E. Barkai, Y. Jung, and R. Silbey *Annual Review of Physical Chemistry* **55**, 457 (2004).
[16] W. P. Ambrose, and W. E. Moerner, *Nature* **349**, 225 (1991).
[17] T. Basche and W. E. Moerner, *Nature* **355**, 335 (1992).
[18] W. E. Moerner, T. Plakhotnik, T. Irngartinger, M. Croci, V. Palm, and U. P. Wild, *Phys. Chem.* **98**, 7382 (1994).
[19] A. M. Boiron, et al *Chem. Phys.* **247** 119 (1999).
[20] K. T. Shimizu, et al *Phys. Rev. Lett.* **89** 117401 (2002)
[21] P. D. Reilly, J. L. Skinner *Phys. Rev. Lett.* **71** 4257 (1993).
[22] E. Geva, and J. L. Skinner, *J. Phys. Chem. B* **101**, 8920 (1997).
[23] P. Bordat, R. Brown *J. of Chemical Physics* **116** 229 (2002).
[24] Y. Tanimura, H. Takano, J. Klafter *J. Chem. Phys.* **108** 1851 (1998).
[25] E. Barkai, Y. Jung, R. Silbey *Phys. Rev. Lett.* **87** 207403 (2001)
[26] Y. Jung, E. Barkai, and R. Silbey *Adv. Chem. Physics* **123**, 199 (2002) and cond-mat/0311428
[27] E. Barkai, A. V. Naumov, Yu. G. Vainer, M. Bauer, L. Kador *Phys. Rev. Lett.* **91** 075502 (2003).
[28] L. Mandel, and E. Wolf, *Optical Coherence and Quantum Optics* (Cambridge University Press, New York, 1995).
[29] H. J. Carmichael *An open System Approach to Quantum Optics* Berlin: Lecture Notes in Physics Springer-Verlag (1993)
[30] M. B. Plenio, and P. L. Knight *Rev. of Mod. Phys.* 70:101–144 (1998).
[31] L. Mandel, *Opt. Lett.* **4** 205 (1979).
[32] R. Short, and L. Mandel, *Phys. Rev. Lett.* **51** 384 (1983).
[33] Th. Basche, W. E. Moerner, M. Orrit, and H. Talon, *Phys. Rev. Lett.* **69**, 1516 (1992).
[34] L. Fleury, J-M. Segura, G. Zumofen, B. Hecht, and U. P. Wild, *Phys. Rev. Lett.* **84**, 1148 (2000).
[35] B. Lounis, H. A. Bechtel, D. Gerion, P. Alivisatos, W. E. Moerner *Chem. Phys. Lett.* **329** 399 (2000).
[36] G. Messin, et al *Optics Letters* **26** 1891 (2001).
[37] F. Treussart, et al *Phys. Rev. Lett.* **89** 093601 (2002).
[38] V. Zwiller, et al *Applied Physics Letters* **78** 2476 (2001).
[39] C. W. Hollars, S. M. Lane, T. Huser *Chem. Phys. Lett.* **370** 393 (2003)
[40] Y. Zheng, F. L. H. Brown *Phys. Rev. Lett.* **90** 238305 (2003)
[41] Y. Zheng, F. L. H. Brown *J. of Chemical Physics* **119** 11814 (2004)
[42] Y. Zheng, F. L. H. Brown *J. of Chemical Physics* **121** 7914 (2004)
[43] P. W. Anderson *J. Phys. Soc. Jpn.* **9** 316 (1954). R. Kubo *ibid* **6** 935 (1954).
[44] R. Kubo, M. Toda, and N. Hashitsume *Statistical Physics 2: Non-Equilibrium Statistical Mechanics* Springer 1978 Berlin.
[45] Y. He, E. Barkai *Phys. Rev. Lett.* **93** 068302 (2004).
[46] H. J. Carmichael, D. F. Walls *J. Phys. B* L43 9 (1976).
[47] H. J. Kimble, M. Dagenais, L. Mandel *Phys. Rev. Lett.* **39** 691 (1977).
[48] J. Dalibard, Y. Castin, and K. Molmer, *Phys. Rev. Lett.* **68** 580 (1992).
[49] S. Mukamel, *Phys. Rev. A* **68** 063821 (2003).
[50] R. J. Cook *Phys. Rev. A* **23** 1241 (1981).
[51] A. I. Burshtein *Sov. Phys. JETP* **22** 937 (1966).
[52] B. W. Shore *The Theory of Coherent Atomic Excitation* Vol. 2, Wiley New-York (1990).
[53] R. Kubo, In *Fluctuations Relaxation and Resonance in Magnetic Systems* D. ter Haar, New York: Plenum (1962).
[54] R. Kubo *Adv. Chem. Phys.* **15** 101 (1969).
[55] B. J. Berne, and R. Pecora *Dynamic Light Scattering* Dover Publication, Chapter 6.
[56] N. G. Kampen, *Stochastic Processes in Physics and Chemistry* North Holland, Amsterdam (1992).